

# Regenerative Role of *Lrig1*<sup>+</sup> Cells in Kidney Repair

Yura Lee <sup>1</sup>, Kwang H. Kim <sup>1</sup>, Jihwan Park <sup>1,2</sup>, Hyun Mi Kang <sup>3</sup>, Sung-Hee Kim <sup>1</sup>, Haengdueng Jeong <sup>1</sup>, Buhyun Lee <sup>1</sup>, Nakyum Lee <sup>1</sup>, Yejin Cho <sup>1</sup>, Gyeong Dae Kim <sup>2</sup>, Seyoung Yu <sup>4</sup>, Heon Yung Gee <sup>4</sup>, Jinwoong Bok <sup>5</sup>, Maxwell S. Hamilton <sup>6</sup>, Leslie Gewin <sup>7,8</sup>, Bruce J. Aronow <sup>9</sup>, Kyung-Min Lim <sup>10</sup>, Robert J. Coffey <sup>6,8</sup> and Ki Taek Nam<sup>1</sup>

## Key Points

- *Lrig1*<sup>+</sup> cells exist long term during kidney homeostasis and become activated upon injury, contributing to regeneration.
- *Lrig1*<sup>+</sup> cells and their progeny emerge during tubulogenesis and contribute to proximal tubule and inner medullary collecting duct development.
- *Lrig1*<sup>+</sup> cells expand and differentiate into a mature nephron lineage in response to AKI to repair the proximal tubule.

## Abstract

**Background** In response to severe kidney injury, the kidney epithelium displays remarkable regenerative capabilities driven by adaptable resident epithelial cells. To date, it has been widely considered that the adult kidney lacks multipotent stem cells; thus, the cellular lineages responsible for repairing proximal tubule damage are incompletely understood. Leucine-rich repeats and immunoglobulin-like domain protein 1-expressing cells (*Lrig1*<sup>+</sup> cells) have been identified as a long-lived cell in various tissues that can induce epithelial tissue repair. Therefore, we hypothesized that *Lrig1*<sup>+</sup> cells participate in kidney development and tissue regeneration.

**Methods** We investigated the role of *Lrig1*<sup>+</sup> cells in kidney injury using mouse models. The localization of *Lrig1*<sup>+</sup> cells in the kidney was examined throughout mouse development. The function of *Lrig1*<sup>+</sup> progeny cells in AKI repair was examined *in vivo* using a tamoxifen-inducible *Lrig1*-specific *Cre* recombinase-based lineage tracing in three different kidney injury mouse models. In addition, we conducted single-cell RNA sequencing to characterize the transcriptional signature of *Lrig1*<sup>+</sup> cells and trace their progeny.

**Results** *Lrig1*<sup>+</sup> cells were present during kidney development and contributed to formation of the proximal tubule and collecting duct structures in mature mouse kidneys. In three-dimensional culture, single *Lrig1*<sup>+</sup> cells demonstrated long-lasting propagation and differentiated into the proximal tubule and collecting duct lineages. These *Lrig1*<sup>+</sup> proximal tubule cells highly expressed progenitor-like and quiescence-related genes, giving rise to a novel cluster of cells with regenerative potential in adult kidneys. Moreover, these long-lived *Lrig1*<sup>+</sup> cells expanded and repaired damaged proximal tubule in response to three types of AKIs in mice.

**Conclusions** These findings highlight the critical role of *Lrig1*<sup>+</sup> cells in kidney regeneration.

JASN 35: 1702–1714, 2024. doi: <https://doi.org/10.1681/ASN.0000000000000462>

This is an open access article distributed under the terms of the [Creative Commons Attribution-Non Commercial-No Derivatives License 4.0 \(CCBY-NC-ND\)](https://creativecommons.org/licenses/by-nc-nd/4.0/), where it is permissible to download and share the work provided it is properly cited. The work cannot be changed in any way or used commercially without permission from the journal.

## Introduction

The kidney is pivotal in removing metabolic waste and regulating volume status. The proximal tubule is the main cellular component of the kidney cortex, responsible for

most solute and water reabsorption from the glomerular filtrate to maintain homeostasis.<sup>1</sup> The proximal tubule epithelium requires high levels of energy and oxidative phosphorylation, rendering this structure vulnerable to

Due to the number of contributing authors, the affiliations are listed at the end of this article.

**Correspondence:** Dr. Ki Taek Nam or Dr. Robert J. Coffey, email: [kitaek@yuhs.ac](mailto:kitaek@yuhs.ac) or [robert.coffey@vumc.org](mailto:robert.coffey@vumc.org)

**Received:** March 6, 2024 **Accepted:** August 5, 2024

**Published Online Ahead of Print:** August 9, 2024

Y.L., K.H.K., and J.P. share co-first authorship.

K.-M.L., R.J.C., and K.T.N. share co-senior authorship.

Present address: Dr. Leslie Gewin, Division of Nephrology, Department of Medicine, Washington University in St. Louis School of Medicine, St. Louis, Missouri

injuries caused by obstructive, ischemic, hypoxic, oxidative, and metabolic insults.<sup>2</sup> Recurrent or severe injury to the proximal tubule epithelium in the context of AKI is a major cause of CKD,<sup>3</sup> affecting over 13% of the global population; treatment options are also limited.

In AKI, the damaged proximal tubule epithelium is reconstituted by proliferative tubule cells<sup>4</sup>; however, their source remains controversial. Some reports suggest that functionally mature cells within the tubule proliferate to repair damage to the proximal tubule.<sup>5</sup> Proximal tubule epithelial cells surviving in AKI dedifferentiate and proliferate to repair the damaged proximal tubule.<sup>3,6–8</sup> By contrast, other studies suggest the existence of distinct wingless-related integration site-responsive,<sup>9,10</sup> SOX9-expressing,<sup>11</sup> and/or protrudin-expressing<sup>12</sup> progenitor populations. However, the cellular lineages responsible for repairing proximal tubule damage are incompletely understood.

Adult quiescent stem cells can be activated upon tissue injury under physiologic conditions. Leucine-rich repeats and immunoglobulin-like domains protein 1 (*Lrig1*) have been identified in the skin,<sup>13</sup> intestine,<sup>14,15</sup> lung,<sup>16</sup> stomach,<sup>17</sup> and oral mucosa<sup>18</sup> of mice as markers for adult epithelial stem cells that are largely quiescent under normal conditions. In the skin, *Lrig1*<sup>+</sup> cells localize to the junctional zone of the hair follicles and contribute to the formation of the entire epidermal lineage.<sup>13</sup> In the intestine, *Lrig1*<sup>+</sup> cells are located in the crypt base and are characterized as a relatively less proliferative<sup>15</sup> but long-lived stem/progenitor cell population, in contrast to the more proliferative *Lgr5*<sup>+</sup> stem/progenitor cells.<sup>19</sup> In the stomach and oral mucosa, *Lrig1* marks long-lived stem cells capable of regenerating the damaged epithelium.<sup>17,18</sup>

*Lrig1* attenuates the downstream signaling cascade induced by activation of the erythroblastic leukemia viral oncogene homologue family of receptor tyrosine kinases by facilitating their ubiquitylation and subsequent lysosomal degradation.<sup>20</sup> *Lrig1* ablation results in increased proliferation of stem cells *in vitro*<sup>21</sup> and epithelial hyperproliferation *in vivo*,<sup>22</sup> supporting that *Lrig1* maintains the quiescent state of adult stem cells. Accordingly, we hypothesized that *Lrig1*<sup>+</sup> cells might be involved in kidney development and tissue regeneration. However, the function and existence of *Lrig1*<sup>+</sup> cells in the kidney remain unknown.

To test this hypothesis, we investigated the localization of *Lrig1*<sup>+</sup> cells in the kidney during the developmental and adult stages of mice, scrutinized the role of *Lrig1*<sup>+</sup> progeny cells in maintaining the kidney tubules and repairing proximal tubule damage induced by AKI in mouse models, and characterized the transcriptional signature of *Lrig1*<sup>+</sup> cells and traced their progeny.

## Methods

### *In Vivo* Lineage Tracing in Mice

All experimental protocols were approved by the Animal Ethics Review Committee of Yonsei University (Institutional Animal Care and Use Committee 2017-0325). Transgenic mice were intraperitoneally injected with

tamoxifen (Sigma-Aldrich; 100 mg/kg, three consecutive days) in corn oil, followed by a single injection of 50 mg/kg 4-hydroxytamoxifen (Sigma-Aldrich) and 1 mg/ml progesterone (Sigma) in corn oil. The detailed procedures for histological analysis are provided in the [Supplemental Material](#) and [Supplemental Table 1](#).

### Single-Cell Capture, Library Preparation, and Single-Cell RNA Sequencing

Tamoxifen-injected *Lrig1*-tdTomato mice were sacrificed at 1 and 365 days after injection. Kidney epithelial cells were isolated for library preparation and single-cell RNA sequencing (scRNA-seq) ([Supplemental Material](#)).

### Kidney Organoid Culture *In Vitro*

For two-dimensional or three-dimensional culture, *Lrig1*-Cre<sup>ERT2</sup> mice were crossed with R26R-TdTomato or B6.129(Cg)-Gt(ROSA)26Sor<sup>tm4</sup>(ACTB-tdTomato-EGFP)<sup>Luo</sup>/J (R26R-ACTB-mT/mG; The Jackson Laboratory, 007676) mice to generate homozygous reporter mice (*Lrig1*-mT/mG mice) expressing membrane-localizing green fluorescent protein (mG). Details regarding the organoid culture and protocol for quantitative polymerase chain reaction of the organoids are provided in the [Supplemental Material](#).

## Results

### *Lrig1*<sup>+</sup> Cells Were Present in the Kidney and Involved in Kidney Epithelial Cell Generation

Immunohistochemistry showed positive LRIG1 expression in the neonatal kidneys; however, positivity rate decreased as the kidney matured. More related details are present in the [Supplemental Material](#) ([Supplemental Figure 1](#)).

One day after tamoxifen administration in *Lrig1*-tdTomato mice ([Figure 1, B and C](#)), tdTomato-expressing single cells were scattered sparsely in the cortex, and their number and clonal size increased over time. One year after tamoxifen administration, some tubules entirely comprised tdTomato<sup>+</sup> cells, indicating that *Lrig1*<sup>+</sup> cell progeny had expanded to constitute the entire cortical tubules ([Figure 1D](#) and [Supplemental Figure 1D](#)). More details are present in the [Supplemental Material](#) ([Supplemental Figure 1, E and F](#)).

Next, we examined whether *Lrig1*<sup>+</sup> cells contribute to kidney development during embryogenesis by administering tamoxifen to pregnant *Lrig1*-tdTomato mice at various stages during embryonic development ([Figure 1G](#)). No tdTomato-expressing cells were detected at E9.5 and E10.5 when the ureteric bud invades the metanephric mesenchyme. However, tdTomato-expressing cells emerged in the tubulogenesis phase (E13.5 and E18.5), and more than 20% of the tubules on both days comprised *Lrig1* progeny ([Figure 1, H–J](#)). These *Lrig1*<sup>+</sup> progeny cells expressed Aquaporin 1<sup>+</sup> lotus tetragonolobus lectin<sup>+</sup> proximal tubule segments at E13.5 and E18.5 ([Figure 2, H and H'](#)) and Aquaporin 2<sup>+</sup> segments of the inner medullary collecting duct at E13.5 ([Figure 2I](#)). *Lrig1*<sup>+</sup> cells and their progeny emerged during tubulogenesis and contributed to the development of proximal tubule and inner medullary collecting ducts.

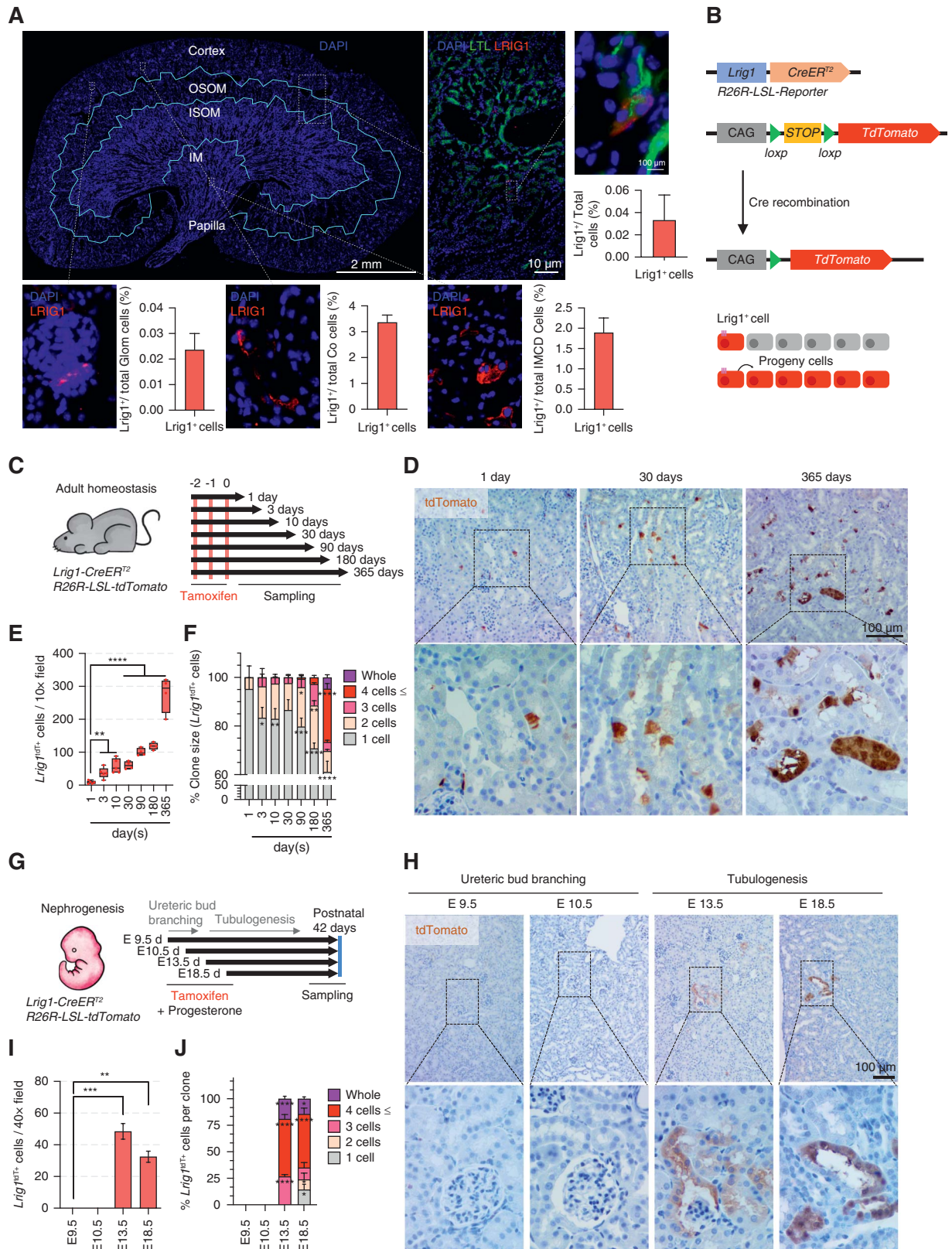


**Figure 1. Presence and lineage tracing of *Lrig1* in the mouse kidney.** (A) LRIG1 expression in the adult kidney (top, left); immunofluorescence images of LRIG1 and the proximal tubule marker LTL, along with quantification of total LRIG1<sup>+</sup>LTL<sup>+</sup> cells (top, right); and *Lrig1* expression levels in the total glomerulus (Glom), cortex (Co), and IM CD for each expression region (bottom). (B) Strategy for generating tamoxifen-inducible *Lrig1*-derived tdTomato labeling *in vivo*. (C) Lineage tracing strategy of *Lrig1*<sup>+</sup> cells and their progeny in the adult kidney. (D) Representative immunohistochemistry images showing *Lrig1*<sup>tdTomo</sup> cells in brown at the indicated days after *Cre-Loxp*

**Figure 1.** *Continued.* recombination. (E) Quantification of tdTomato<sup>+</sup> cells on days 1, 3, 10, 30, 90, 180, and 365 ( $N=4$  mice, 112 images). Significance was tested using one-way ANOVA. (F) Quantification of tdTomato<sup>+</sup> clone size at the indicated times plotted as the percentage of the total number of clones ( $N=4$  mice, 448 images). Significance was tested using two-way ANOVA. (G) Lineage tracing strategy of *Lrig1*<sup>+</sup> cells and their progeny during nephrogenesis. (H) Representative immunohistochemistry images showing *Lrig1*-tdTomato<sup>+</sup> cells in brown at the indicated embryonic dates to P46 in the *Cre-Loxp* recombination-induced kidney ( $N=3$ , 48 images). (I) Quantification of tdTomato<sup>+</sup> cells at the indicated dates. Significance was tested using one-way ANOVA. (J) tdTomato<sup>+</sup> clone sizes quantified at the indicated tracing times and plotted as the percentage of the total number of clones. Significance was tested using two-way ANOVA. All results are presented as mean  $\pm$  SD. \* $P < 0.05$ , \*\* $P < 0.01$ , \*\*\* $P < 0.001$ , \*\*\*\* $P < 0.0001$ . DAPI, 4',6-diamidino-2-phenylindole; IM CD, inner medullary collecting duct; LTL, lotus tetragonolobus lectin.

We immunostained sections of the tamoxifen-treated *Lrig1*-tdTomato mouse kidney with antibodies against specific nephron lineage markers (Supplemental Figure 2A) to identify the specific cell types derived from *Lrig1*<sup>+</sup> cells. At 365 days after *Cre-Loxp* recombination, tdTomato<sup>+</sup> cells were positive for lotus tetragonolobus lectin and Aquaporin 1, consistent with those in the proximal tubule (Figure 2A). They also colocalized with desmin<sup>+</sup> cells in the glomerulus, consistent with the patterns of mesangial cells (Figure 2B). *Lrig1*<sup>tdTomato+</sup> cells were not observed in the other nephron lineages, such as the Cal-D28K<sup>+</sup> distal convoluted tubule (Figure 2C), Aquaporin 2<sup>+</sup> or anion exchange protein 1 (AE1)<sup>+</sup> connecting tubule (Figure 2, D and D'), CLCK1<sup>+</sup> thin loop of Henle (Figure 2E), and Tamm-Horsfall glycoprotein<sup>+</sup> thin and thick loops of Henle (Figure 2F). Time-course observations revealed that *Lrig1*<sup>tdTomato+</sup> cells progressively expanded to form the lotus tetragonolobus lectin<sup>+</sup> Aquaporin 1<sup>+</sup> proximal tubule over 180 days. In the inner medullary collecting duct, Aquaporin 2<sup>+</sup> principal cells and AE1<sup>+</sup>  $\alpha$ -intercalated cells were labeled with tdTomato (Figure 2G and Supplemental Figure 2, C and D). In the nephron tubules isolated 1 year after *Lrig1-Cre* recombination, the *Lrig1*<sup>tdTomato+</sup> cells had expanded in a longitudinal direction, forming an entire tubular segment (Figure 2J). *Lrig1*<sup>tdTomato+</sup> clones were observed, starting as single cells on day 1, expanding in both the horizontal and vertical directions (Figure 2, K and L), and eventually forming entire tubules (Figure 2M).

### *Lrig1*<sup>+</sup> Cells Repaired Proximal Tubule Damage from Various Kidney Injury Types

After high-dose folic acid-induced AKI (Figure 3A), the kidneys showed severe tubular damage with loss of the brush border, dilation of the lumen, and a necrotic tubular epithelium (Figure 3B). After injury, *Lrig1*<sup>+</sup> cells survived and increased in the high-dose folic acid-induced AKI model; however, on day 7 of ongoing repair, their numbers decreased to the baseline (Supplemental Figure 3A). Subsequently, the clonal size of *Lrig1*<sup>tdTomato+</sup> cells significantly expanded in the high-dose folic acid group (Figure 3C), whereas the number of clones was unchanged. *Lrig1*<sup>tdTomato+</sup> cells costained with kidney injury molecule-1, a marker of injured kidney cells (Figure 3D), and colocalized with the lotus tetragonolobus lectin<sup>+</sup> or Aquaporin 1<sup>+</sup> proximal tubule. Damaged cortical *Lrig1*<sup>tdTomato+</sup> cells did not express Calbindin-D28k, whereas *Lrig1*<sup>+</sup> progeny costained with Aquaporin 2<sup>+</sup> and AE1<sup>+</sup> cells, indicating their expansion in the damaged proximal tubule and inner medullary collecting duct regions (Supplemental Figure 3B). In the

recovery phase, the number of tdTomato<sup>+</sup> lotus tetragonolobus lectin<sup>+</sup> cells increased dramatically (Figure 3E).

Similar to the high-dose folic acid-induced AKI model, unilateral ischemia/reperfusion injury and unilateral ureteral obstruction injury showed extensive tubular injury with flattened tubule cells, tubular casts, and necrotic tubular cells (Supplemental Figure 3, C, D, F, and G); larger tdTomato<sup>+</sup> clones were detected in the KIM-1<sup>+</sup> damaged tubules than in the sham control (Supplemental Figure 3, E and H).

### *Lrig1*<sup>+</sup> Progeny Cells Exhibited Self-Renewal and Long-Term Propagation

*Lrig1*<sup>+</sup> cells in the adult kidney and intestine were predominantly quiescent, as indicated by low coexpression with Ki-67 and 5-bromo-2'-deoxyuridine (Supplemental Figure 4). More details are present in the Supplemental Material.

Kidney organoids were prepared from *Lrig1*-mT/mG mice after tamoxifen treatment (Figure 4G) to trace the *Lrig1*<sup>mG+</sup> cells (Figure 4H and Supplemental Figure 5). In the initial culture, mT<sup>+</sup> and *Lrig1*<sup>mG+</sup> kidney cells coexisted (Figure 4I, P0), whereas only *Lrig1*<sup>mG+</sup> cells survived over time (Figure 4I, P14). *Lrig1*<sup>mG+</sup> cells formed organoids with at least a 20- $\mu$ m diameter (Figure 4J). Quantitative polymerase chain reaction showed that *Lrig1*<sup>mG+</sup> organoids expressed *Lrig1*, along with other nephron progenitor markers (*Sall1*, *Six2*, *Foxo1*, *Cited1*, and *Ors1*) and ureteric epithelium markers (*Hoxp7* and *Gata3* but not *Wt1* and *cRET*<sup>23</sup>) (Figure 4K and Supplemental Table 2).

We confirmed that cells constituting the *Lrig1*<sup>mG+</sup> organoids were part of the kidney lineage through PAX8 protein expression (Figure 4L). *Lrig1*<sup>mG+</sup> organoids were costained with Aquaporin 2<sup>+</sup> CD cells (Figure 4M) and Megalin<sup>+</sup> proximal tubule cells (Figure 4N), suggesting that *Lrig1*<sup>+</sup> progeny could differentiate into a mature nephron lineage with capacity to generate different lineages of kidney cells.

### scRNA-Seq Profile of *Lrig1*<sup>+</sup> Cells

We explored the molecular landscape and cellular dynamics of *Lrig1*<sup>+</sup> cells by scRNA-seq of kidney epithelial cells from the *Lrig1*-tdTomato mice at days 1 and 365 (Figure 5A) to elucidate the subpopulation existing within the kidney alongside the tubule cells. At day 1, 20.2% of total kidney cells were identified as tdTomato<sup>+</sup> cells, which increased to 26.9% by day 365 (Figure 5B). Unsupervised clustering of total kidney cells identified 17 cell clusters, further defined according to reported sets of cell type-specific markers on the basis of the expression of more than 14 differentially expressed genes (DEGs), identified on the basis of an adjusted  $P$  value  $< 0.01$  and

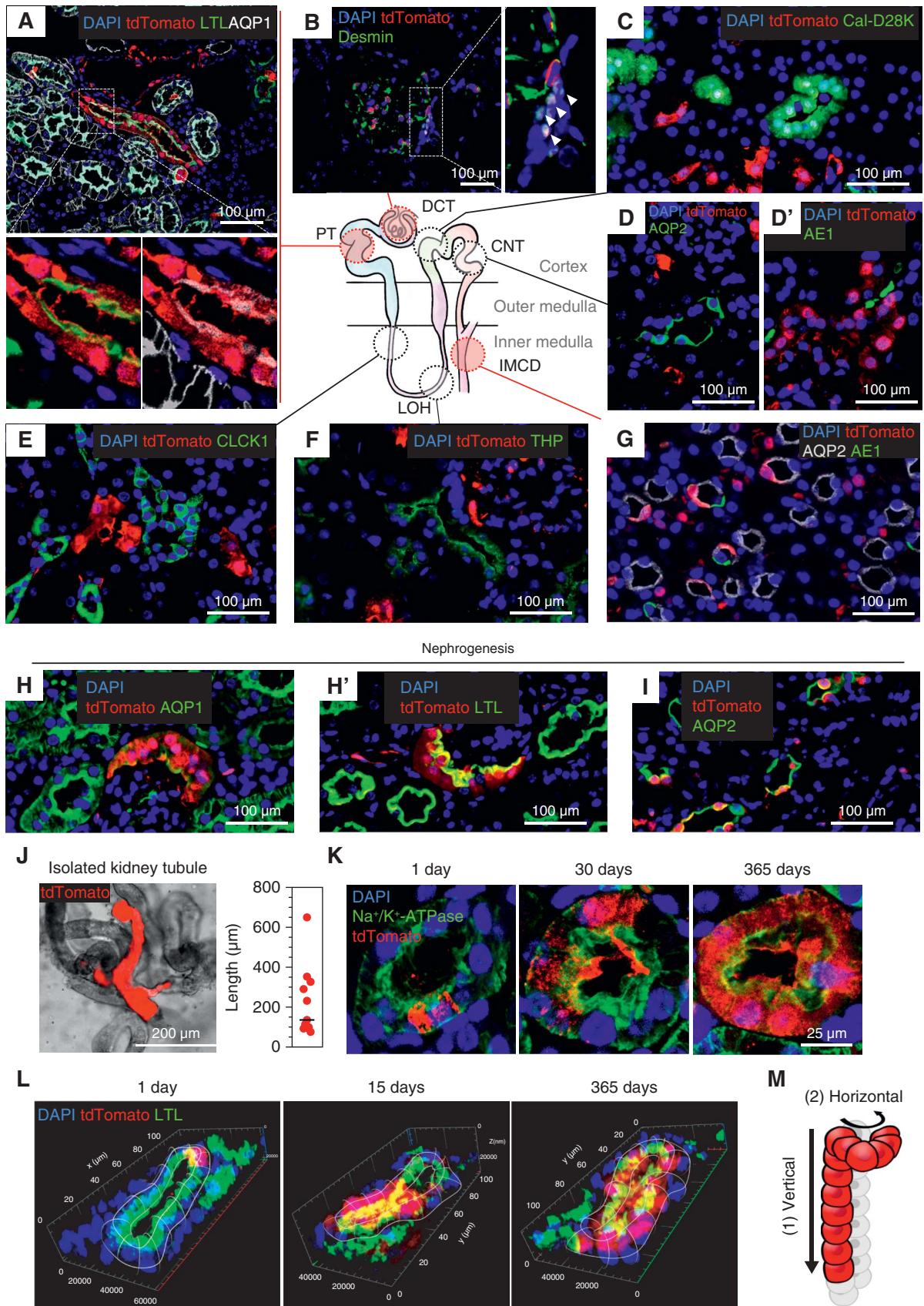


**Figure 2. Identification of kidney tissues constructed by *Lrig1*<sup>+</sup> cells and their progeny.** Immunofluorescence images of tdTomato<sup>+</sup> cells and nephron tubular markers in the PT (LTL, Aquaporin 1) (A), mesangial cell (desmin) (B), DCT (CalbindinD28K [Cal-D28K]) (C),

**Figure 2.** *Continued.* CNT (Aquaporin 2 [D], AE1 [D']), LOH (CLCK1 [E], THP [F]), and CD (Aquaporin 2, AE1) (G). (H and I) Kidney sections from E18.5 of *Lrig1*-tdTomato mice stained for tdTomato and nephron tubule markers. (J) Isolated tubule obtained at day 365 after *Cre* recombination showing *Lrig1*<sup>tdT+</sup> cells expanded longitudinally. The graph shows the tdTomato<sup>+</sup> tubule length ( $\mu\text{m}$ ) from isolated tubules. (K) *Lrig1*<sup>tdT+</sup> cells in the isolated tubule immunofluorescence stained with Na<sup>+</sup>/K<sup>+</sup>-ATPase on days 1, 30, and 365. (L) Z-stack reconstituted immunofluorescent image of tdTomato (red) and LTL (green) in the kidney on days 1, 15, and 365. (M) Graphical image of the tdTomato<sup>+</sup> cell division in the longitudinal (1) and horizontal (2) directions of the tubule. AE1, anion exchange protein 1; CNT, connecting tubule; DCT, distal convoluted tubule; LOH, loop of Henle; PT, proximal tubule.

average log fold change >1 (Figure 5C and Supplemental Figure 6A). These clusters included cells with relatively higher mitochondria content that were associated with solute carrier transporter protein-expressing cells, such

as those in the proximal tubule and distal tubule.<sup>24</sup> The portion of the proximal tubule (PT) cluster significantly increased (34%–56%) from day 1 to day 365 (Figure 5D). The transcriptomes of *Lrig1*<sup>+</sup> cells were only sparsely

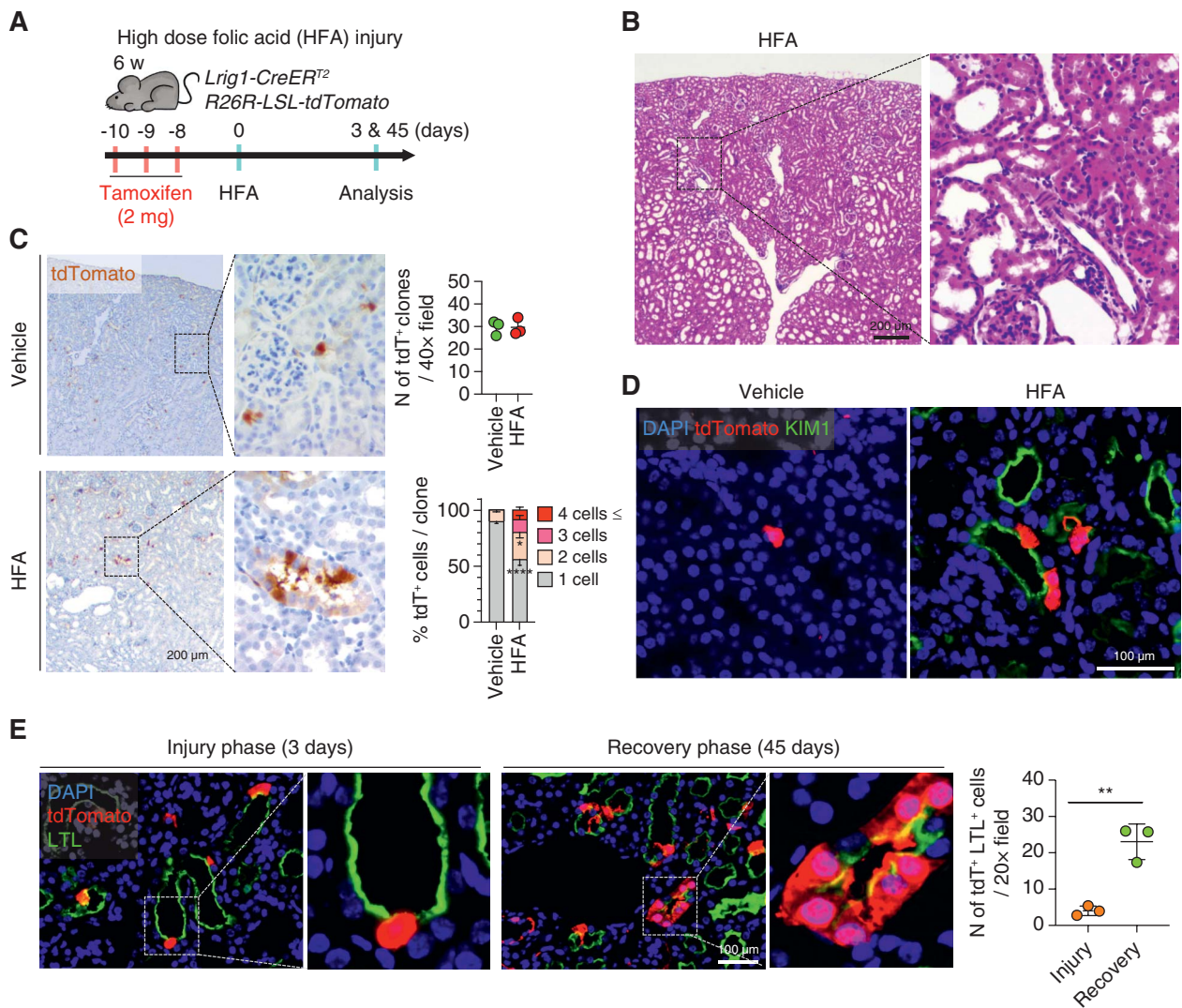


**Figure 3. Tracing of *Lrig1*<sup>+</sup> cells and their progeny during the injury and recovery phases.** (A) Schematic image of HFA (250 mg/kg)-induced AKI in *Lrig1*-tdTomato mice. The kidney was collected 3 and 45 days after HFA treatment. (B) Hematoxylin and eosin-stained images of HFA-induced AKI in *Lrig1*-tdTomato cells. Representative immunohistochemistry images showing *Lrig1*<sup>tdT+</sup> cells in brown. (C) The numbers of tdTomato<sup>+</sup> clones were counted in 40 $\times$  fields. The tdTomato<sup>+</sup> clone size was quantified and plotted as the percentage of the total number of clones ( $N=6$  mice, 322 images). Significance was tested using Student's unpaired *t* test and two-way ANOVA. (D) Immunofluorescence images of *Lrig1*<sup>tdT+</sup> cells (red), KIM-1 (green), and DAPI (blue). (E) Immunofluorescence images of *Lrig1*<sup>tdT+</sup> cells and Aquaporin 1 and LTL as PT markers in the injury and recovery phases. All results are presented as mean  $\pm$  SD. \* $P < 0.05$ , \*\* $P < 0.01$ , \*\*\* $P < 0.0001$ . HFA, high-dose folic acid; KIM-1, kidney injury molecule-1.

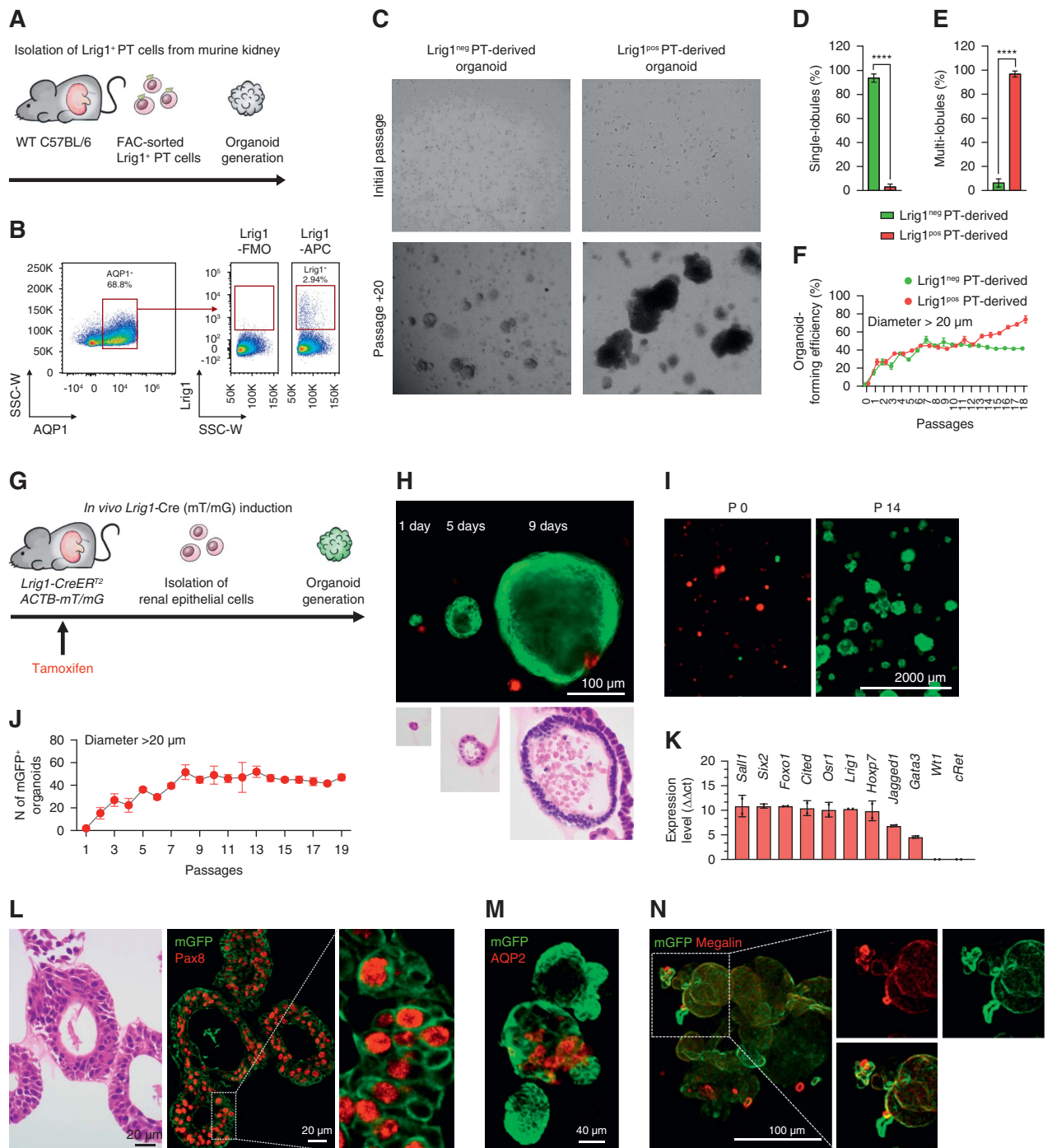


**Figure 4. Self-renewal and stemness of *Lrig1*<sup>+</sup>-derived cells *in vitro*.** (A) Fluorescence-activated cell sorting isolation of *Lrig1*<sup>+</sup> PT cells and organoid generation scheme. (B) Flow cytometry of the WT kidney with FMO or *Lrig1*<sup>APC+</sup>; Aquaporin 1<sup>APC/Cy7+</sup> cells. (C) Representative images of *Lrig1*<sup>+</sup> and *Lrig1*<sup>-</sup> PT organoids at the initial stage and after 20 passages. (D and E) Quantification of single-lobular (D) and multilobular (E) organoids. (F) Quantification of organoid-forming efficiency of *Lrig1*<sup>+</sup> and *Lrig1*<sup>-</sup> organoids. (G) The *Cre-LoxP* recombinase induction scheme *in vivo* using *Lrig1-Cre*<sup>ERT2-R26R-mT/mG</sup> mice and kidney organoid generation. (H) Representative images of *Lrig1*<sup>mGFP+</sup> kidney organoids cultured for 0, 5, and 9 days. (I) Images of *Lrig1*<sup>mGFP+</sup> kidney organoids maintained over passage 14. (J) Quantification of 1–19 consecutive passages of mGFP<sup>+</sup> kidney organoids with diameters >20  $\mu$ m. (K) Relative mRNA expression of *Lrig1* and kidney embryonic stem cell genes in *Lrig1*<sup>mGFP+</sup> organoids. (L) Hematoxylin and eosin-stained images of *Lrig1*<sup>mGFP+</sup> organoids and paraffin-sanctioned *Lrig1*<sup>mGFP+</sup> organoid staining with PAX8. (M and N) Whole-mount staining of *Lrig1*<sup>mGFP+</sup> organoids with Aquaporin 2 (red) (M) or megalin (N). All results are presented as mean  $\pm$  SD. \*\*\*\**P* < 0.0001. FAC, fluorescence-activated cell; FMO, fluorescence minus one; SSC-W, side scatter pulse width; WT, wild-type.

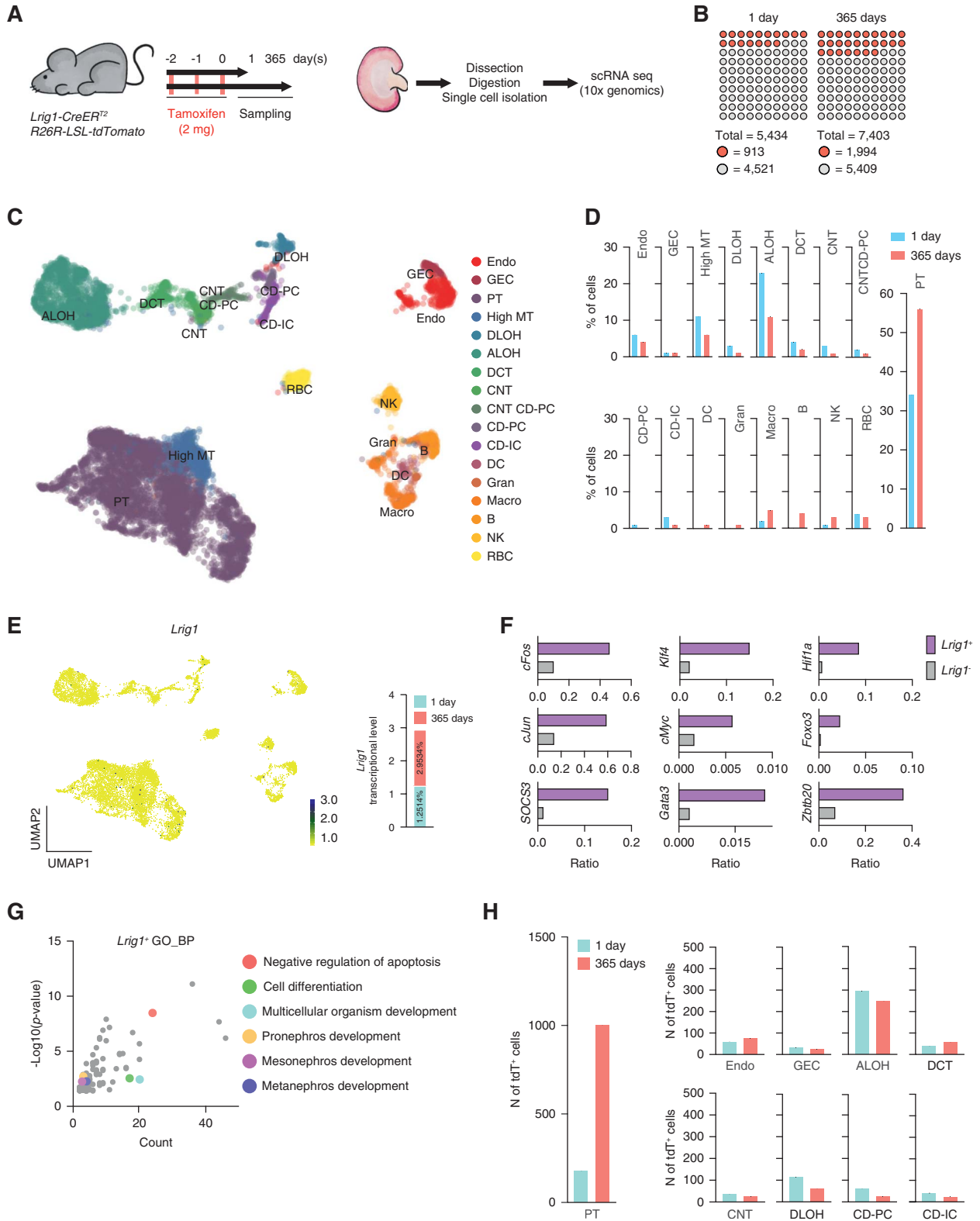


**Figure 5. scRNA-seq of *Lrig1*<sup>+</sup> cell-derived tdTomato<sup>+</sup> cells in the kidney.** (A) Schematic of the scRNA-seq analysis experimental design. *Cre-Loxp* recombination-induced *Lrig1*-tdTomato<sup>+</sup> mouse kidneys were collected on days 1 and 365. (B) The number of single cells collected from the kidneys at days 1 and 365. Red dots: *Lrig1*-tdTomato<sup>+</sup> cells; white dots: *Lrig1*-tdTomato<sup>-</sup> cells. (C) UMAP plot of scRNA-seq data. Seventeen distinct cell populations identified are colored by cell-type clusters: ENDO, GEC, PT, high MT, DLOH, ALOH, DCT, CNT, CNT CD-PC, CD-PC, CD-IC, DC, Gran, Macro, B, NK, RBC. (D) Percentage of total number of cells in each cluster of day 1 and day 365 kidneys. (E) Relative expression of *Lrig1* from the lowest (yellow dots) to highest (navy dots) levels on days 1 and 365 presented in a UMAP plot. (F) Ratio of stem cell-related gene-expressing cells in *Lrig1*<sup>+</sup> and *Lrig1*<sup>-</sup> cells. (G) GO analysis of DEGs showing the top 136

**Figure 5.** *Continued.* significant GO terms (biological processes) associated with the *Lrig1*<sup>+</sup> DEGs. (H) Numbers of tdTomato<sup>+</sup> cells in the nephron cluster in the day 1 and day 365 kidneys. ALOH, ascending loop of Henle; B, B cells; CD-IC, collecting duct intercalated cells; CD-PC, collecting duct principal cells; CNT CD-PC, CNT-collecting duct principal cells; DC, dendritic cells; DEG, differentially expressed gene; DLOH, descending loop of Henle; ENDO, endothelial cells; GEC, glomerular epithelial cell; GO, gene ontology; Gran, granulocytes; high MT, high mitochondrial cells in the PT; Macro, macrophages; NK, natural killer cells; RBC, red blood cell; scRNA-seq, single-cell RNA sequencing; UMAP, uniform manifold approximation and projection.

detected across multiple clusters, exhibiting low expression levels, consistent with immunohistochemistry (Figure 5E).

*Lrig1*<sup>+</sup> cells showed high expression of genes associated with differentiation (*Krt8*, *Krt18*), lipid metabolism (*pyruvate dehydrogenase kinase 4*, *Malat1*), and quiescence (*Tob1*, *Btg2*, and *Klf6*) (Supplemental Figure 6B). *Lrig1*<sup>+</sup> cells highly expressed *cFos*, *cJun*, and *Socs3*, which regulate somatic stem cell renewal<sup>25,26</sup>; *Klf4*, *cMyc*, and *Gata3*, associated with reprogramming of stemness<sup>27</sup>; and *Hif1α*, *Foxo3*, and *Zbtb20*, which are expressed in quiescent stem cells<sup>28</sup> (Figure 5F) compared with *Lrig1*<sup>-</sup> cell populations. Gene ontology analysis of the DEGs revealed that *Lrig1*<sup>+</sup> cell populations were enriched in genes involved in the antiapoptotic pathway, cell differentiation, and development-associated pathways (Figure 5G). More details are present in the Supplemental Material (Supplemental Figure 6, C–I).

Next, we traced tdTomato<sup>+</sup> cells in day 1 and day 365 kidneys to examine the role of *Lrig1*<sup>+</sup> progeny in the long-term maintenance of the proximal tubule. tdTomato<sup>+</sup> cells were widely distributed in nearly all kidney lineages, including an immune cell cluster (Figure 5G). Although there was no difference in the proportion of tdTomato<sup>+</sup> cells in most kidney clusters, the PT cluster showed a five-fold increase in the number of tdTomato<sup>+</sup> cells on day 365 (Figure 5H), consistent with *in vivo* lineage tracing of the cortex (Figure 1), further demonstrating that *Lrig1*<sup>+</sup> progeny may contribute to long-term maintenance of proximal tubule.

### Enrichment of *Lrig1*<sup>+</sup> Cells and Their Progeny in a Novel Stem Cell Niche of Adult Kidney Proximal Tubule

As shown in Figure 5H, tdTomato<sup>+</sup> cells showed the greatest increase in the day 365 PT cluster. The PT cluster was divided into four subclusters (Figure 6A) on the basis of the known sets of cell type-specific markers, including *Slc5a12*, *Slc5a2*, and *Slc13a3* for PT<sup>S1</sup>; *Ddah1* for PT<sup>S2</sup>; and *Slc16a9* and *Slc7a13* for PT to identify the tdTomato<sup>+</sup>-enriched cluster.<sup>53</sup> PT<sup>S1</sup> and PT<sup>S2</sup> clusters comprise fully differentiated PT cells,<sup>24</sup> whereas the PT<sup>S3</sup> cluster comprises a label-retaining cell population that recycles slowly in the rat kidney.<sup>29</sup>

We discovered a novel subcluster in the day 365 PT cluster, comprising proximal tubule quiescent progenitors, designated PT<sup>QPs</sup>. The PT<sup>QPs</sup> cluster showed higher expression levels of pyruvate dehydrogenase kinase 4 and cysteine-rich protein 61 (*Cyr61*), upregulated in AKI<sup>30,31</sup> (Figure 6B), than those of the other PT subclusters, suggesting its role in kidney regeneration. The ratio of PT<sup>S3</sup> decreased with age, corresponding with the stem cell niche characteristic.<sup>32</sup> The ratio and total cell number of PT<sup>QPs</sup> increased with age (Figure 6, C and D). More

related results are present in the Supplemental Material (Supplemental Figure 7).

We performed immunofluorescent staining for JunD, KLF6, and CYR61 in kidney sections because their encoding genes were among the top 10 DEGs compared with other PT clusters (Figure 6E) to determine specific markers for PT<sup>QPs</sup>. JunD and CYR61 were not expressed in proximal tubule populations (data not shown), whereas KLF6 was specifically stained in the PT and costained with lotus tetragonolobus lectin markers (Figure 6F). KLF6 expression increased in lotus tetragonolobus lectin<sup>+</sup>KLF6<sup>+</sup> cells by day 365 compared with that detected on day 1 (Figure 6G), supporting the increase in the PT<sup>QPs</sup> population in the proximal tubule on day 365.

### *Lrig1*<sup>+</sup> PT<sup>QPs</sup> Were Mainly Responsible for the Regeneration of the Adult Kidney

We compared the composition of tdTomato-expressing cells in each PT cluster on day 1 and day 365 to track the changes in *Lrig1*<sup>+</sup> progeny in the PT clusters. The proportion of tdTomato<sup>+</sup> cells increased in the PT<sup>QPs</sup> and PT<sup>S2</sup> clusters at day 365 compared with that at day 1, whereas this population decreased in PT<sup>S3</sup> and was unchanged in PT<sup>S1</sup> (Figure 6, H and I), suggesting that *Lrig1*<sup>+</sup> progeny in PT<sup>S3</sup> contribute to forming proximal tubule mainly at younger ages, whereas the role of *Lrig1*<sup>+</sup> progeny in PT<sup>QPs</sup> becomes more dominant with age. We analyzed the trajectories of single cells according to their progression toward differentiation to test this hypothesis. Combining the data for day 1 and day 365 samples, the PT<sup>S3</sup> and PT<sup>QPs</sup> clusters branched into two distinct trajectories toward PT<sup>S1</sup> (Figure 6J). The day 1 trajectory showed that PT<sup>S3</sup> predominantly differentiated into the PT<sup>S1</sup> cluster, whereas the PT<sup>QPs</sup> cluster mainly contributed to the PT<sup>S1</sup> cluster cells on day 365 (Figure 6K). Alignment of the trajectories demonstrated that tdTomato-expressing cells in the PT<sup>S3</sup> cluster predominantly differentiated into PT<sup>S1</sup> on day 1, whereas those in the PT<sup>QPs</sup> cluster mainly contributed to PT<sup>S1</sup> on day 365 (Figure 6L). Immunofluorescent staining showed that KLF6<sup>+</sup> cells (the marker for PT<sup>QPs</sup>) colocalized with tdTomato-expressing tubules, and the proportion of these KLF6<sup>+</sup> tdTomato<sup>+</sup> tubules significantly increased from day 1 to day 365 (Figure 6, M and N). Our data support that *Lrig1*<sup>+</sup> PT<sup>QPs</sup> cells are responsible for the regeneration of the mature kidney.

### Transcriptomic Profiling of *LRIG1*<sup>+</sup> Human Kidney Cells

Finally, we assessed *LRIG1* expression in adult human kidney cells using a public scRNA-seq database.<sup>33</sup> More

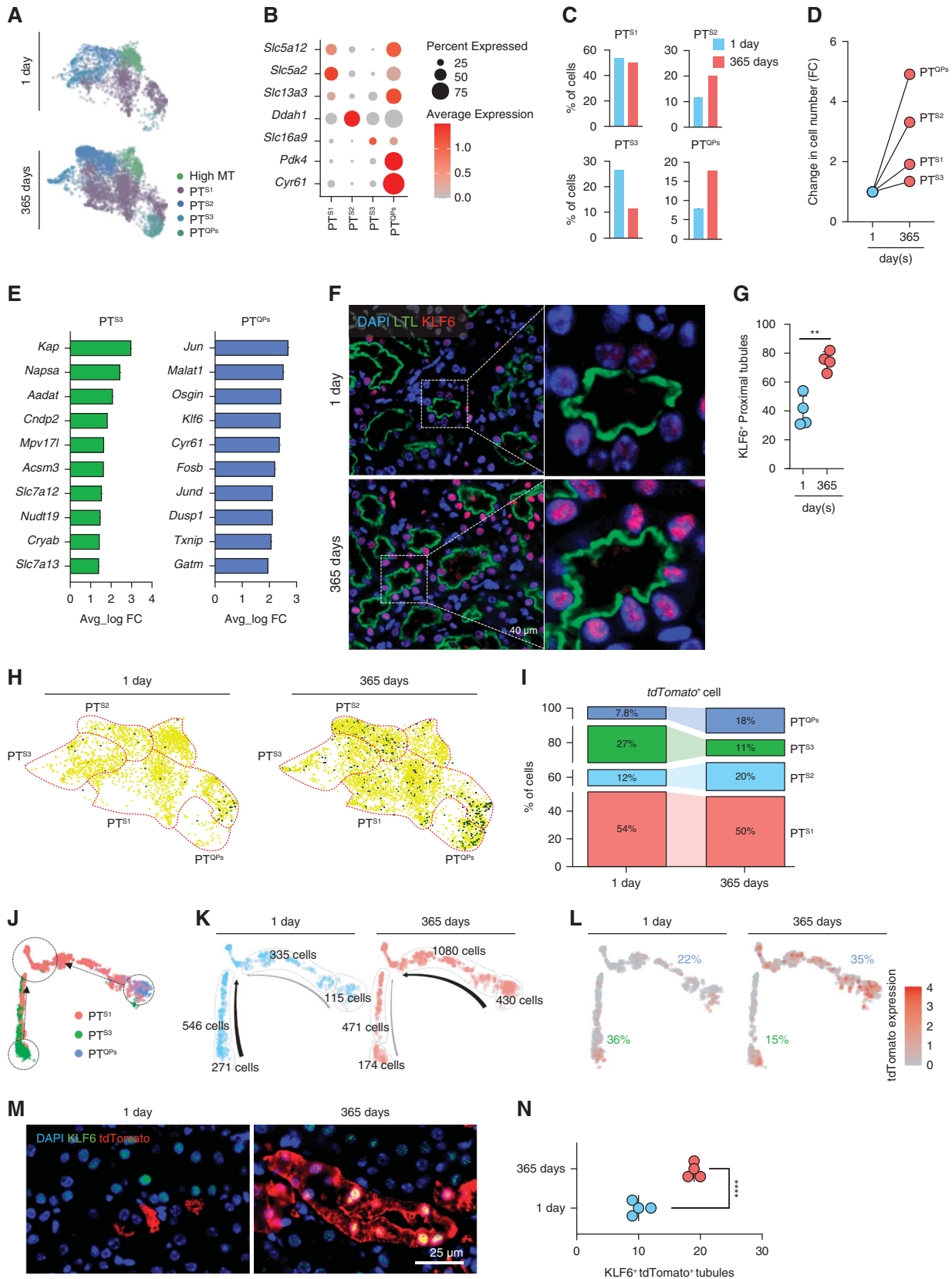


**Figure 6. Subclustering of the PT cluster and identification of the novel PT<sup>QPs</sup> cluster.** (A) UMAP plot of PT subclusters. (B) Bubble plot showing the expression of PT-specific genes in PT subclusters. (C) Percentage of PT subcluster cells on days 1 to 365. (D) Quantification graph showing FC values from day 1 to 365 in each cluster. (E) Top ten highly expressed genes in the PT<sup>S3</sup> (green) and PT<sup>QPs</sup> (blue) clusters. (F) Immunofluorescence staining for LTL (PT marker) and KLF6 in day 1 and day 365 kidney sections. (G) Quantification of LTL<sup>+</sup>KLF6<sup>+</sup> cells

**Figure 6.** *Continued.* per 20× field in day 1 and day 365 kidney sections ( $N=3$ , 24 images). (H) Relative expression of tdTomato<sup>+</sup> cells in the PT clusters with the lowest (yellow dots) to highest (navy dots) expression levels on days 1 and 365. (I) Proportions (%) of tdTomato<sup>+</sup> cells in each PT cluster at days 1 and 365. (J) Pseudotime trajectory divided into three states by Monocle. The PT<sup>S1</sup>, PT<sup>S3</sup>, and PT<sup>QPs</sup> clusters were used for ordering and are plotted with different colors. Black arrows represent the pseudotime direction. (K) tdTomato<sup>+</sup> cells plotted in a trajectory graph on days 1 and 365 after *Cre-Loxp* recombination induction or (L) colored in a gradient from the lowest (gray dots) to highest (red dots) expression levels. (M) Immunofluorescence staining for tdTomato<sup>+</sup> and KLF6 in day 1 and day 365 kidney sections. (N) Quantification of tdTomato<sup>+</sup> KLF6<sup>+</sup> cells per 20× field in day 1 and day 365 kidney sections ( $N=5$ , 42 images). Significance was evaluated using Student's unpaired *t* test. \*\* $P < 0.01$ , \*\*\*\* $P < 0.0001$ . FC, fold change.

details related to this section are present in the Supplemental Material (Supplemental Figure 8).

## Discussion

*Lrig1* was expressed in the embryonic and adult mouse kidney. Lineage tracing revealed that *Lrig1*<sup>+</sup> cells and their progeny constituted proximal tubule, mesangial cells in the glomerulus, and principal/ $\alpha$ -intercalated cells in the inner medullary collecting duct. In the proximal tubule, *Lrig1*<sup>+</sup> cells comprise a population of largely quiescent cells that proliferate and contribute to the repair of proximal tubule damage after AKI.

The sources of cells contributing to the repair of proximal tubule damage after kidney injury, Chang-Panesso and Humphreys<sup>3</sup> suggested that the regenerating cells are the surviving tubular epithelial cells. This was supported by the coexpression of *Slc34a1*,<sup>7</sup> along with markers of dedifferentiation, proliferation, and progenitor cells, rather than the emergence of new immature cells.

A recent study<sup>34</sup> demonstrated that mature cells can undergo dedifferentiation; express progenitor-associated genes, such as *Sox9*<sup>11,35</sup>; and proliferate during recovery from injury, a phenomenon termed "paligenosis."<sup>34</sup> However, another group proposed the involvement of a distinct progenitor cell population for kidney regeneration. Protrudin<sup>+</sup> cells may mark a kidney progenitor cell population.<sup>12</sup> They compared the regenerative capacity of protrudin<sup>+</sup> cells with that of cells expressing *Rosa26* in an AKI damage model.<sup>12</sup> Although *Rosa26*<sup>+</sup> cells reconstituted 80% of the tubules, protrudin<sup>+</sup> cells reacted earlier to kidney injury, suggesting a role of kidney progenitor cells in kidney repair. These conflicting results might stem from the experimental limitation of the lineage tracing systems used in these previous studies, which focused on a single gene marker, thereby limiting the ability to monitor the dynamics of entire genes.

We demonstrated that *Lrig1*<sup>+</sup> cells express mature proximal tubule markers along with various gene sets associated with adult stem cells by combining tdTomato lineage tracing systems with scRNA-seq analysis. This showed that *Lrig1*<sup>+</sup> cells in the proximal tubule act as mature and functional tubule cells, which harbor progenitor cell capacity, thereby actively participating in kidney repair and maintenance. A similar phenomenon has been suggested in the stomach. There are two stem cell zones: the isthmus and base regions. In contrast to the isthmus that shows rapidly cycling stem cells, the base chief cells slowly cycle and express mature markers, such as gastric intrinsic factor and pepsinogen. These cells are enriched with secretory granules containing digestive enzymes.

However, adult stem cell markers—*Lgr5*, *Troy*, and *Lrig1*—mark gastric intrinsic factor<sup>+</sup> chief cells, and these cells can transdifferentiate and proliferate when necessary.<sup>36</sup> These studies suggest that progenitor-like markers coexist with mature cell markers in organs like the stomach, and similar patterns might also be observed in fully mature kidneys. *Lrig1*<sup>+</sup> cells and their progeny did not express with kidney adult progenitors, suggesting that *Lrig1*<sup>+</sup> cell represents a novel cell population that is committed to the regeneration of the proximal tubule. This finding indicates that rather than depending on a single progenitor cell, heterogeneous progenitor cell may participate in maintaining the kidney.

*Lrig1* regulates the quiescence and self-renewal of neuronal stem cells by inhibiting epidermal growth factor receptor signaling in the brain.<sup>37–40</sup> LRIG1 negatively regulates the erythroblastic leukemia viral oncogene homologue family by associating with receptor tyrosine kinases and promoting their degradation.<sup>20</sup> We speculated that *Lrig1* maintained the quiescence in the kidney, and silencing of *Lrig1* could activate epidermal growth factor receptor, thereby inducing cell proliferation.

Our study has limitations because of the lack of research on the function of individual *Lrig1*<sup>+</sup> cells as a progenitor population. Therefore, analyses, such as multi-ome analysis, are needed to investigate the role of individual *Lrig1*<sup>+</sup> cells. In addition, it is necessary to verify the effect of *Lrig1*<sup>+</sup> cell ablation on kidney homeostasis and the repair of damaged epithelial cells.

We demonstrated the existence of a *Lrig1*<sup>+</sup> quiescent cell population in the proximal tubule and its pivotal role in the regeneration of kidney proximal tubule. These findings provide important insight into the mechanisms underlying proximal tubule repair, which can guide the development of a therapeutic strategy to treat kidney injury.

## Disclosures

Disclosure forms, as provided by each author, are available with the online version of the article at <http://links.lww.com/JSN/E810>.

## Funding

K.T. Nam: Korea Mouse Phenotyping Project (RF-2016M3A9D5A01952416), the Ministry of Science and ICT (MSIT) of the Government of South Korea (RS-2023-00241446, 2022R1A2C3007850, and 2022M3A9F3016364), and the Ministry of Trade, Industry, and Energy, Korea (MOTIE) industrial innovation infrastructure construction project (P0021516). J. Park: Basic Science Research Program through the National Research Foundation of Korea (NRF-2019R1C1C1005403). L. Ge-win: Department of Veterans Affairs Merit Review Award

(1I01BX003425-01A21). R.J. Coffey: National Cancer Institute (R35 CA197570 and P50 CA236733) and the Nicholas Tierney Memorial GI Cancer Fund. K.-M. Lim: the National Research Foundation (NRF, 2018R1A5A2025286).

#### Author Contributions

**Conceptualization:** Robert J. Coffey, Kyung-Min Lim, Ki Taek Nam.

**Data curation:** Bruce J. Aronow, Kwang H. Kim, Sung-Hee Kim, Jihwan Park.

**Formal analysis:** Hyun Mi Kang, Yura Lee, Jihwan Park.

**Funding acquisition:** Sung-Hee Kim, Ki Taek Nam.

**Investigation:** Jinwoong Bok, Robert J. Coffey, Heon Yung Gee, Leslie Gewin, Haengdueng Jeong, Kwang H. Kim, Sung-Hee Kim, Buhyun Lee, Yura Lee.

**Methodology:** Yejin Cho, Haengdueng Jeong, Hyun Mi Kang, Sung-Hee Kim, Buhyun Lee, Nakyum Lee, Seyoung Yu.

**Project administration:** Ki Taek Nam.

**Resources:** Jinwoong Bok, Heon Yung Gee, Leslie Gewin, Maxwell S. Hamilton, Hyun Mi Kang, Gyeong Dae Kim, Jihwan Park.

**Software:** Gyeong Dae Kim.

**Validation:** Yejin Cho, Maxwell S. Hamilton, Nakyum Lee, Jihwan Park.

**Visualization:** Kwang H. Kim, Yura Lee.

**Writing – original draft:** Robert J. Coffey, Yura Lee, Kyung-Min Lim, Ki Taek Nam.

**Writing – review & editing:** Yura Lee, Kyung-Min Lim, Ki Taek Nam.

#### Data Sharing Statement

Previously published data used for this study were deposited in the Gene Expression Omnibus (GEO) under accession code GSE107585. Raw data supporting this study's findings are openly available at the Korea Bioinformatics Center (KOBIC; <https://www.kobic.re.kr/kobic/>) under reference number PRJKA220138.

#### Supplemental Material

This article contains the following supplemental material online at <http://links.lww.com/JSN/E809>.

[Supplemental Methods.](#)

[Supplemental Figure 1.](#) Presence and lineage tracing of *Lrig1* in the mouse kidney.

[Supplemental Figure 2.](#) Identification of *Lrig1*<sup>+</sup> cell-derived tubules in the mouse kidney.

[Supplemental Figure 3.](#) *Lrig1*<sup>+</sup> cells and their progeny expand after AKI.

[Supplemental Figure 4.](#) *Lrig1*<sup>+</sup> cells and their progeny are slowly cycling and long-lived in adult kidneys.

[Supplemental Figure 5.](#) Self-renewal and stemness of *Lrig1*<sup>+</sup>-derived cells *in vitro*.

[Supplemental Figure 6.](#) Phenotype and functional characterization of *Lrig1*<sup>+</sup> cells.

[Supplemental Figure 7.](#) Characteristics of the PT<sup>QPs</sup> cluster.

[Supplemental Figure 8.](#) Expression of *LRIG1* in human kidney tissue and genetic characteristics of *LRIG1*<sup>+</sup> cells.

[Supplemental Table 1.](#) Primary antibodies used in this study.

[Supplemental Table 2.](#) Primer sequences used in this study.

#### References

- Chang-Panesso M, Kadyrov FF, Lalli M, et al. FOXM1 drives proximal tubule proliferation during repair from acute ischemic kidney injury. *J Clin Invest.* 2019;129(12):5501–5517. doi:10.1172/JCI125519
- Chevalier RL. The proximal tubule is the primary target of injury and progression of kidney disease: role of the glomerulotubular junction. *Am J Physiol Renal Physiol.* 2016;311(1):F145–F161. doi:10.1152/ajprenal.00164.2016
- Chang-Panesso M, Humphreys BD. Cellular plasticity in kidney injury and repair. *Nat Rev Nephrol.* 2017;13(1):39–46. doi:10.1038/nrneph.2016.169
- Bonventre JV, Yang L. Cellular pathophysiology of ischemic acute kidney injury. *J Clin Invest.* 2011;121(11):4210–4221. doi:10.1172/JCI45161
- Humphreys BD, Valerius MT, Kobayashi A, et al. Intrinsic epithelial cells repair the kidney after injury. *Cell Stem Cell.* 2008;2(3):284–291. doi:10.1016/j.stem.2008.01.014
- Humphreys BD, Czerniak S, DiRocco DP, Hasnain W, Cheema R, Bonventre JV. Repair of injured proximal tubule does not involve specialized progenitors. *Proc Natl Acad Sci U S A.* 2011;108(22):9226–9231. doi:10.1073/pnas.1100629108
- Kusaba T, Lalli M, Kramann R, Kobayashi A, Humphreys BD. Differentiated kidney epithelial cells repair injured proximal tubule. *Proc Natl Acad Sci U S A.* 2014;111(4):1527–1532. doi:10.1073/pnas.1310653110
- Berger K, Bangen JM, Hammerich L, et al. Origin of regenerating tubular cells after acute kidney injury. *Proc Natl Acad Sci U S A.* 2014;111(4):1533–1538. doi:10.1073/pnas.1316177111
- Barker N, Rookmaaker MB, Kujala P, et al. Lgr5(+ve) stem/progenitor cells contribute to nephron formation during kidney development. *Cell Rep.* 2012;2(3):540–552. doi:10.1016/j.celrep.2012.08.018
- Schutgens F, Rookmaaker MB, Blokzijl F, et al. Troy/TNFRSF19 marks epithelial progenitor cells during mouse kidney development that continue to contribute to turnover in adult kidney. *Proc Natl Acad Sci U S A.* 2017;114(52):E11190–E11198. doi:10.1073/pnas.1714145115
- Kang HM, Huang S, Reidy K, Han SH, Chinga F, Susztak K. Sox9-Positive progenitor cells play a key role in renal tubule epithelial regeneration in mice. *Cell Rep.* 2016;14(4):861–871. doi:10.1016/j.celrep.2015.12.071
- Oliver JA, Sampogna RV, Jalal S, et al. A subpopulation of label-retaining cells of the kidney papilla regenerates injured kidney medullary tubules. *Stem Cell Rep.* 2016;6(5):757–771. doi:10.1016/j.stemcr.2016.03.008
- Jensen KB, Collins CA, Nascimento E, et al. *Lrig1* expression defines a distinct multipotent stem cell population in mammalian epidermis. *Cell Stem Cell.* 2009;4(5):427–439. doi:10.1016/j.stem.2009.04.014
- Wong VW, Stange DE, Page ME, et al. *Lrig1* controls intestinal stem-cell homeostasis by negative regulation of ErbB signalling. *Nat Cell Biol.* 2012;14(4):401–408. doi:10.1038/ncb2464
- Powell AE, Wang Y, Li Y, et al. The pan-ErbB negative regulator *Lrig1* is an intestinal stem cell marker that functions as a tumor suppressor. *Cell.* 2012;149(1):146–158. doi:10.1016/j.cell.2012.02.042
- Succony L, Gomez-Lopez S, Pennycuik A, et al. *Lrig1* expression identifies airway basal cells with high proliferative capacity and restricts lung squamous cell carcinoma growth. *Eur Respir J.* 2022;59(3):2000816. doi:10.1183/13993003.00816-2020
- Choi E, Lantz TL, Vlachich G, et al. *Lrig1*<sup>+</sup> gastric isthmal progenitor cells restore normal gastric lineage cells during damage recovery in adult mouse stomach. *Gut.* 2018;67(9):1595–1605. doi:10.1136/gutjnl-2017-313874
- Byrd KM, Piehl NC, Patel JH, et al. Heterogeneity within stratified epithelial stem cell populations maintains the oral mucosa in response to physiological stress. *Cell Stem Cell.* 2019;25(6):814–829.e6. doi:10.1016/j.stem.2019.11.005
- Sato T, Vries RG, Snippert HJ, et al. Single Lgr5 stem cells build crypt-villus structures *in vitro* without a mesenchymal niche. *Nature.* 2009;459(7244):262–265. doi:10.1038/nature07935
- Segatto O, Anastasi S, Alema S. Regulation of epidermal growth factor receptor signalling by inducible feedback inhibitors. *J Cell Sci.* 2011;124(Pt 11):1785–1793. doi:10.1242/jcs.083303
- Jensen KB, Watt FM. Single-cell expression profiling of human epidermal stem and transit-amplifying cells: *Lrig1* is a regulator

- of stem cell quiescence. *Proc Natl Acad Sci U S A*. 2006; 103(32):11958–11963. doi:10.1073/pnas.0601886103
22. Wang Y, Shi C, Lu Y, Poulin EJ, Franklin JL, Coffey RJ. Loss of *Lrig1* leads to expansion of Brunner glands followed by duodenal adenomas with gastric metaplasia. *Am J Pathol*. 2015; 185(4):1123–1134. doi:10.1016/j.ajpath.2014.12.014
  23. Combes AN, Phipson B, Lawlor KT, et al. Single cell analysis of the developing mouse kidney provides deeper insight into marker gene expression and ligand-receptor crosstalk. *Development*. 2019;146(12):dev178673. doi:10.1242/dev.178673
  24. Park J, Shrestha R, Qiu C, et al. Single-cell transcriptomics of the mouse kidney reveals potential cellular targets of kidney disease. *Science*. 2018;360(6390):758–763. doi:10.1126/science.aar2131
  25. Pargin M, Giubolini S, Barone C, et al. *Ssox2* controls neural stem cell self-renewal through a *Fos*-centered gene regulatory network. *Stem Cells*. 2021;39(8):1107–1119. doi:10.1002/stem.3373
  26. Biteau B, Hochmuth CE, Jasper H. Maintaining tissue homeostasis: dynamic control of somatic stem cell activity. *Cell Stem Cell*. 2011;9(5):402–411. doi:10.1016/j.stem.2011.10.004
  27. Ben-David U, Nissenbaum J, Benvenisty N. New balance in pluripotency: reprogramming with lineage specifiers. *Cell*. 2013;153(5):939–940. doi:10.1016/j.cell.2013.04.051
  28. Cheung TH, Rando TA. Molecular regulation of stem cell quiescence. *Nat Rev Mol Cell Biol*. 2013;14(6):329–340. doi:10.1038/nrm3591
  29. Vogetseder A, Palan T, Bacic D, Kaissling B, Le Hir M. Proximal tubular epithelial cells are generated by division of differentiated cells in the healthy kidney. *Am J Physiol Cell Physiol*. 2007; 292(2):C807–C813. doi:10.1152/ajpcell.00301.2006
  30. Oh CJ, Ha CM, Choi YK, et al. Pyruvate dehydrogenase kinase 4 deficiency attenuates cisplatin-induced acute kidney injury. *Kidney Int*. 2017;91(4):880–895. doi:10.1016/j.kint.2016.10.011
  31. Feng D, Ngov C, Henley N, Boufaied N, Gerarduzzi C. Characterization of matricellular protein expression signatures in mechanistically diverse mouse models of kidney injury. *Sci Rep*. 2019;9(1):16736. doi:10.1038/s41598-019-52961-5
  32. Liu QZ, Chen XD, Liu G, Guan GJ. Identification and isolation of kidney-derived stem cells from transgenic rats with diphtheria toxin-induced kidney damage. *Exp Ther Med*. 2016;12(3): 1651–1656. doi:10.3892/etm.2016.3516
  33. Wu H, Uchimura K, Donnelly EL, Kirita Y, Morris SA, Humphreys BD. Comparative analysis and refinement of human PSC-derived kidney organoid differentiation with single-cell transcriptomics. *Cell Stem Cell*. 2018;23(6):869–881.e8. doi:10.1016/j.stem.2018.10.010
  34. Willet SG, Lewis MA, Miao ZF, et al. Regenerative proliferation of differentiated cells by mTORC1-dependent paligenesis. *EMBO J*. 2018;37(7):e98311. doi:10.15252/embj.201798311
  35. Kumar S, Liu J, Pang P, et al. *Sox9* activation highlights a cellular pathway of renal repair in the acutely injured mammalian kidney. *Cell Rep*. 2015;12(8):1325–1338. doi:10.1016/j.celrep.2015.07.034
  36. Liabeuf D, Oshima M, Stange DE, Sigal M. Stem cells, *Helicobacter pylori*, and mutational landscape: utility of preclinical models to understand carcinogenesis and to direct management of gastric cancer. *Gastroenterology*. 2022;162(4):1067–1087. doi:10.1053/j.gastro.2021.12.252
  37. Marques-Torreson MA, Williams CAC, Southgate B, et al. *LRIG1* is a gatekeeper to exit from quiescence in adult neural stem cells. *Nat Commun*. 2021;12(1):2594. doi:10.1038/s41467-021-22813-w
  38. Jeong D, Lozano Casasbuenas D, Gengatharan A, et al. *LRIG1*-Mediated inhibition of EGF receptor signaling regulates neural precursor cell proliferation in the neocortex. *Cell Rep*. 2020; 33(2):108257. doi:10.1016/j.celrep.2020.108257
  39. Lee J, Lee J, Choi C, Kim JH. Blockade of integrin  $\alpha 3$  attenuates human pancreatic cancer via inhibition of EGFR signalling. *Sci Rep*. 2019;9(1):2793. doi:10.1038/s41598-019-39628-x
  40. Yan Y, Yan H, Wang Q, Zhang L, Liu Y, Yu H. MicroRNA 10a induces glioma tumorigenesis by targeting myotubularin-related protein 3 and regulating the Wnt/ $\beta$ -catenin signaling pathway. *FEBS J*. 2019;286(13):2577–2592. doi:10.1111/febs.14824

## AFFILIATIONS

- <sup>1</sup>Department of Biomedical Sciences, Brain Korea 21 PLUS Project for Medical Science, Yonsei University College of Medicine, Seoul, Korea
- <sup>2</sup>School of Life Sciences, Gwangju Institute of Science and Technology (GIST), Gwangju, Korea
- <sup>3</sup>Stem Cell Research Center, Korea Research Institute of Bioscience and Biotechnology, Daejeon, Korea
- <sup>4</sup>Department of Pharmacology, Brain Korea 21 PLUS Project for Medical Science, Yonsei University College of Medicine, Seoul, Korea
- <sup>5</sup>Department of Anatomy, Brain Korea 21 PLUS Project for Medical Science, Yonsei University College of Medicine, Seoul, Korea
- <sup>6</sup>Epithelial Biology Center and Department of Medicine, Vanderbilt University School of Medicine, Nashville, Tennessee
- <sup>7</sup>Division of Nephrology and Hypertension, Department of Medicine and Cell and Developmental Biology, Vanderbilt University School of Medicine, Nashville, Tennessee
- <sup>8</sup>Department of Medicine, Veterans Affairs Hospital, Tennessee Valley Healthcare System, Nashville, Tennessee
- <sup>9</sup>Departments of Biomedical Informatics, Developmental Biology, and Pediatrics, Cincinnati Children's Hospital Medical Center, Cincinnati, Ohio
- <sup>10</sup>College of Pharmacy, Ewha Womans University, Seoul, Korea